Supplementation

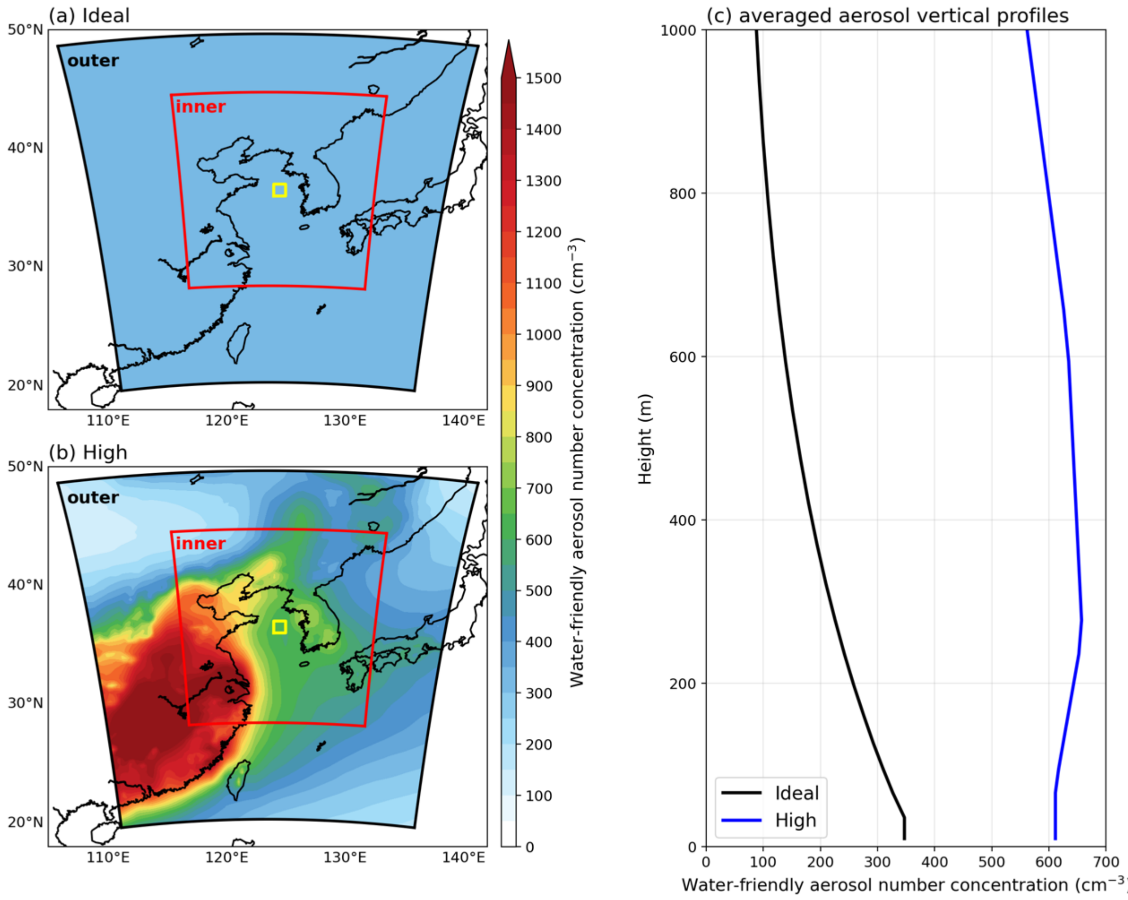

Figure S1. (a) Idealized and (b) high water-friendly aerosol number concentration (shaded in cm^{-3}) at the lowest model level. The black and red quadrilaterals indicate the outer and inner simulation domains, respectively. (c) Vertical profiles of water-friendly aerosol number concentration for the idealized (black line) and high-aerosol (blue line) configurations, averaged over the yellow rectangle shown in (a) and (b). The high-aerosol field is obtained by uniformly scaling the default WRF climatological aerosol field by a factor of 0.1.

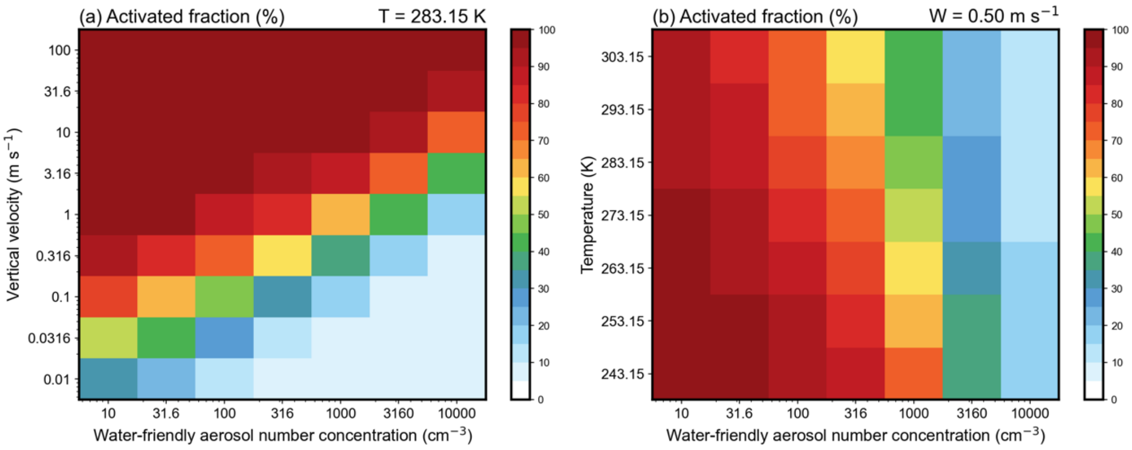

Figure S2. (a) Activated fraction (shaded in %) as a function of water-friendly aerosol number concentration and vertical velocity at a temperature of 283.15 K. (b) Activated fraction (shaded in %) as a function of water-friendly aerosol number concentration and temperature at a vertical velocity of 0.5 m s^{-1}.

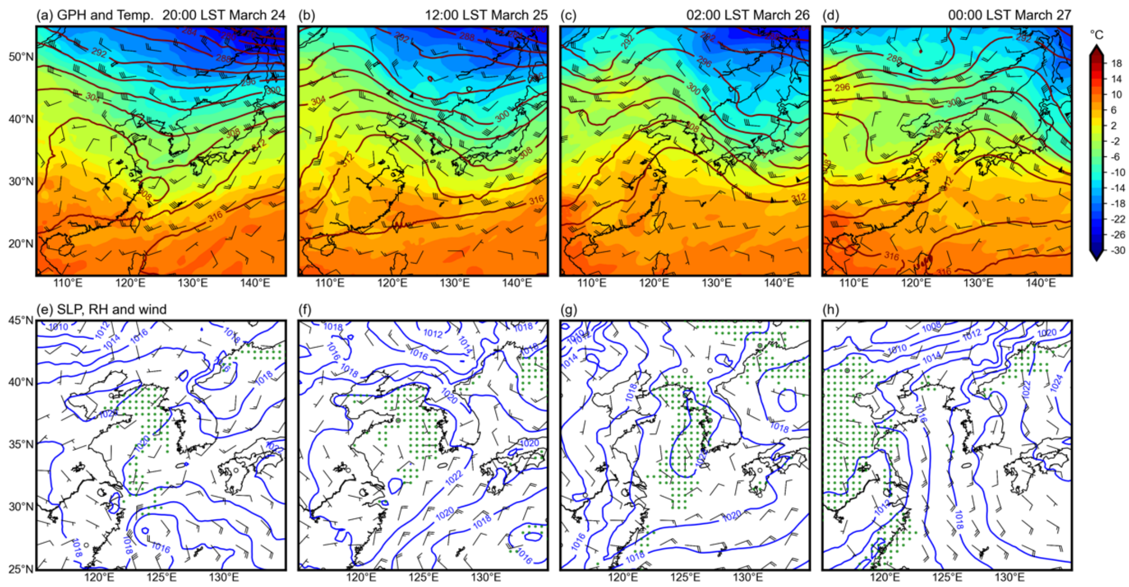

Figure S3. (a-d) 850-hPa geopotential height (contours at 40-gpm interval), winds (barbs in m s^{-1}) and temperature (shaded in °C). (e-h) Sea level pressure (contours at 4-hPa interval), 10-m winds (barbs in m s^{-1}) and surface relative humidity exceeding 90% (green dots). The four columns are at 20:00 LST on March 24, 12:00 LST on March 25, 02:00 LST on March 26 and 00:00 LST on March 27, respectively.

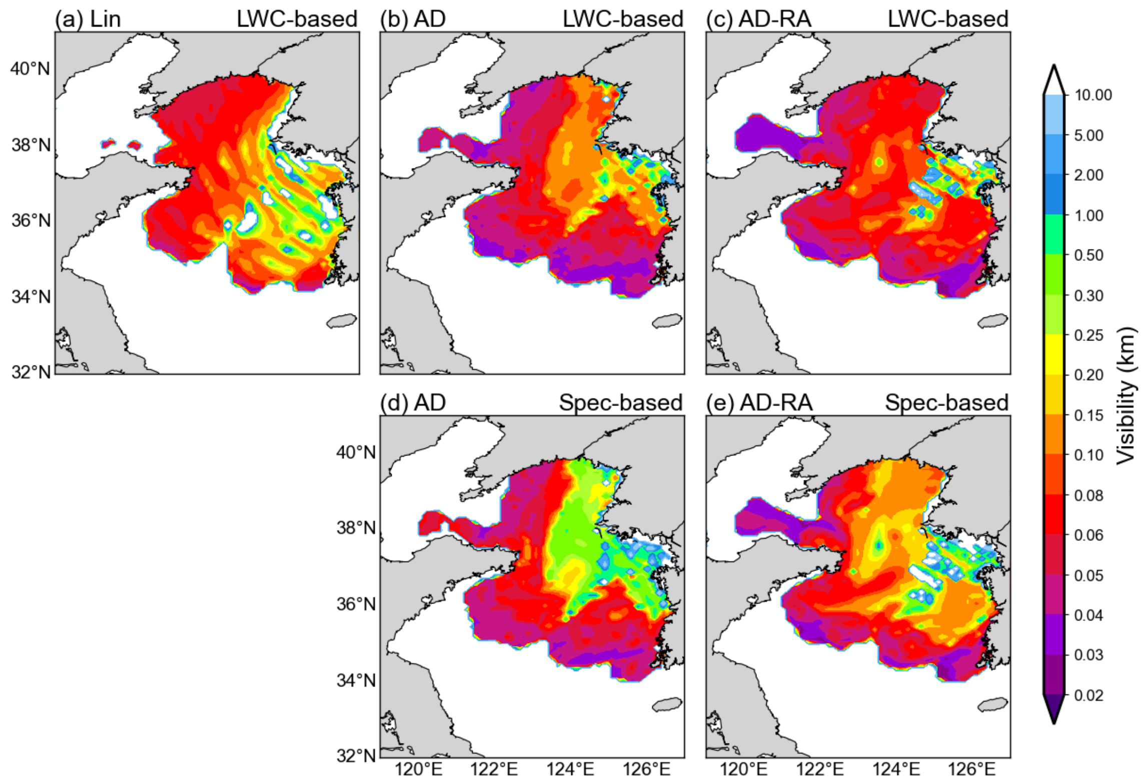

Figure S4. Simulated 10-m visibility (shaded in km) at 07:00 LST on March 25. (a-c) show visibility diagnosed using the formulation of Kunkel (1984) for the Lin, AD, and AD-RA experiments, respectively. (d) and (e) show visibility diagnosed using a spectral method based on Mie theory and the predicted cloud droplet size distributions for the AD and AD-RA experiments, respectively.

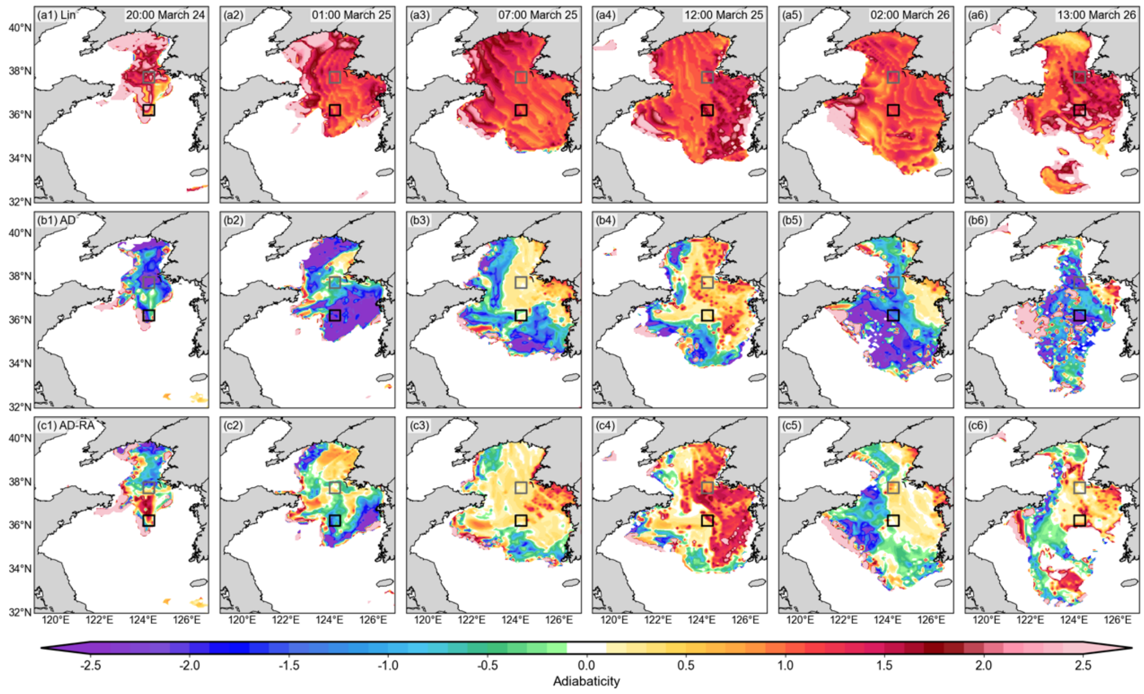

Figure S5. Simulated adiabaticity (shading in unit 1) from the (row a) Lin, (b) AD, and (c) AD-RA experiments, respectively. Columns 1-6 correspond to 20:00 LST on March 24, 01:00, 07:00, and 12:00 LST on March 25, and 02:00 and 13:00 LST on March 26, respectively. The black rectangles mark the region (124–124.5° E, 36–36.5° N) used for Fig. S6. The gray rectangles mark the region (124–124.5° E, 37.5–38° N) selected for the liquid water budget analysis presented in Figs. S7-S9.

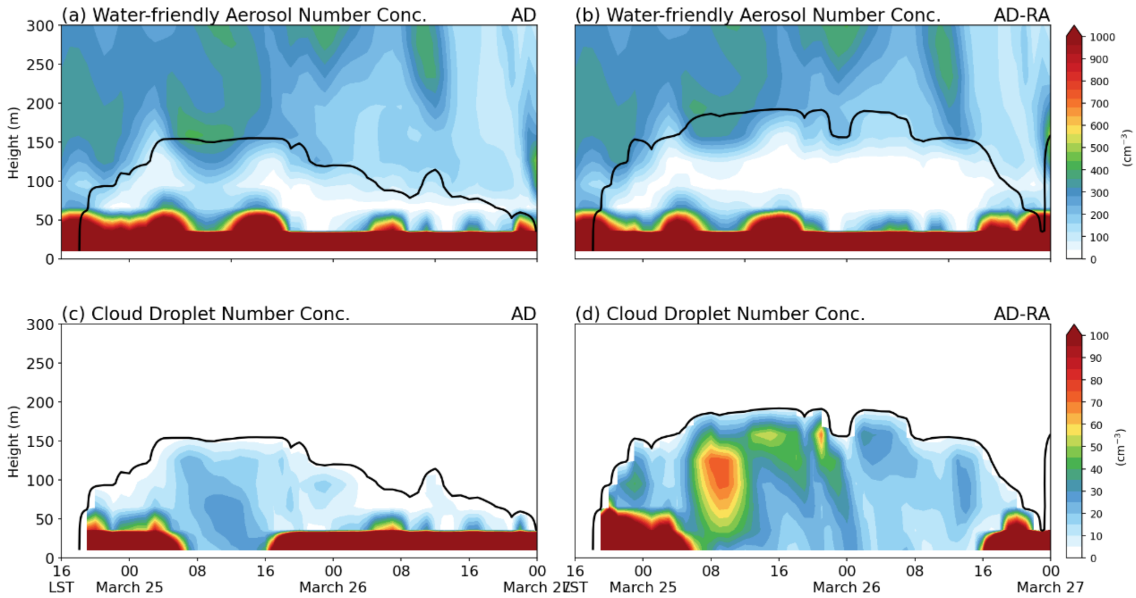

Figure S6. Area-averaged time-height distributions of (a, b) water-friendly aerosol number concentration (shaded in cm^{-3}), and (c, d) cloud droplet number concentration (shaded in cm^{-3}) over the region marked by the black rectangles in Fig. S5. The left and right columns correspond to the AD and AD-RA experiments. Black contours denote the LWC threshold of 0.016 g m^{-3}.

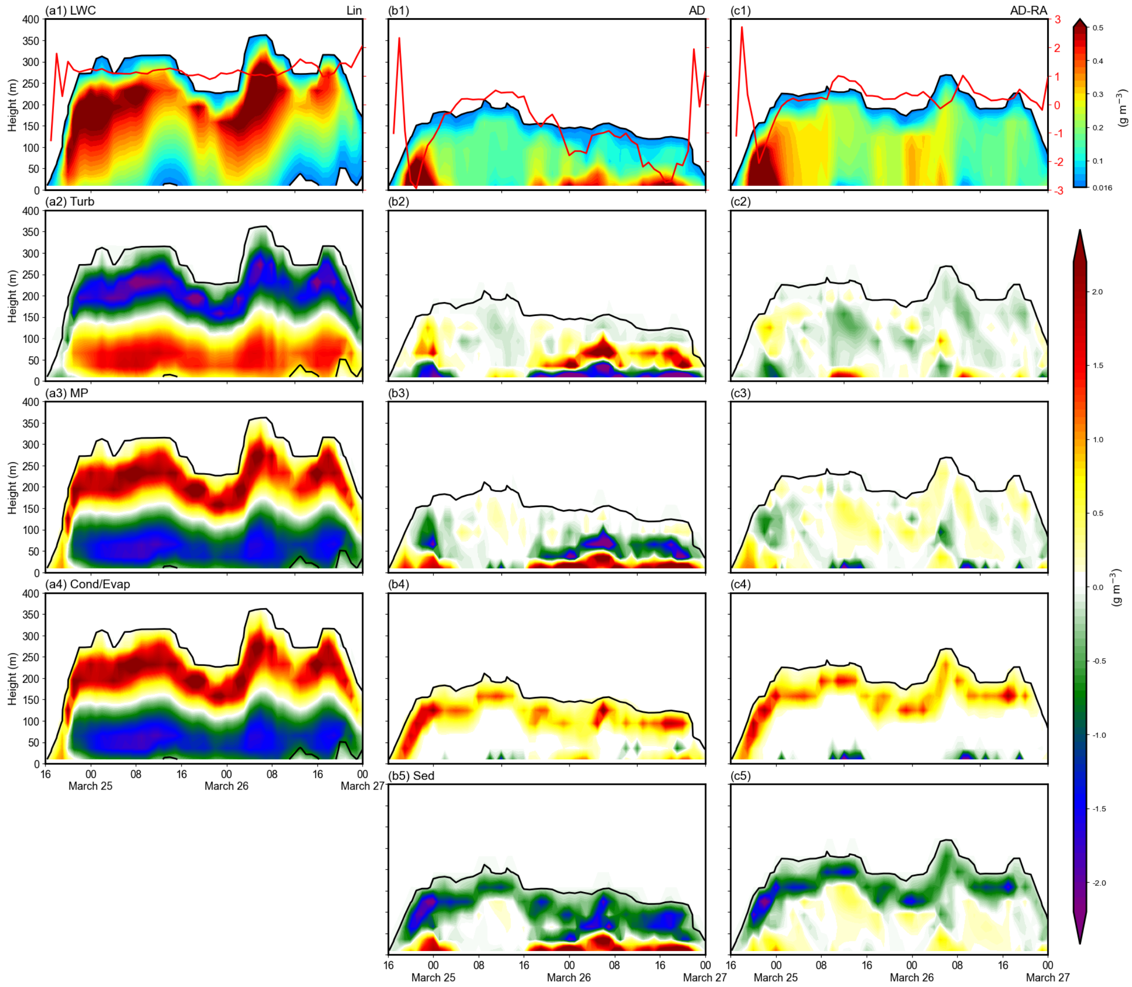

Figure S7. Area-averaged time-height distributions of the LWC budget terms over the region marked by the gray rectangles in Fig. S5. Columns (a), (b), and (c) correspond to the Lin, AD, and AD-RA experiments, respectively. Within each column, rows 1-5 show the total LWC change and the contributions from turbulence, microphysics, condensation-evaporation, and sedimentation. Black contours denote the LWC threshold of 0.016 g m^{-3}. (b5) and (c5) show the sedimentation contribution because it is the dominant component among sedimentation, autoconversion, and accretion in the AD and AD-RA experiments.

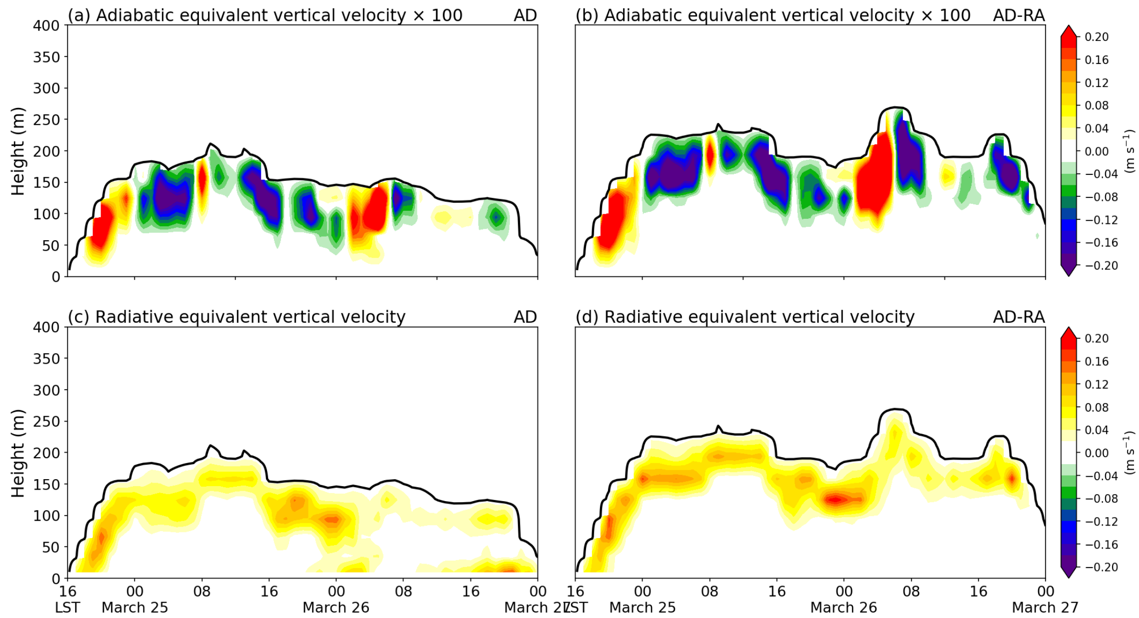

Figure S8. Area-averaged time-height distributions of (a, b) adiabatic equivalent vertical velocity (shaded in m s^{-1}) multiplied by 100, and (c, d) radiative equivalent vertical velocity (shaded in m s^{-1}) over the region marked by the gray rectangles in Fig. S5. The left and right columns correspond to the AD and AD-RA experiments. Black contours denote the LWC threshold of 0.016 g m^{-3}. An equivalent vertical velocity magnitude of 0.15 m s^{-1} corresponds to a temperature change rate magnitude of approximately 0.05 K min^{-1}.

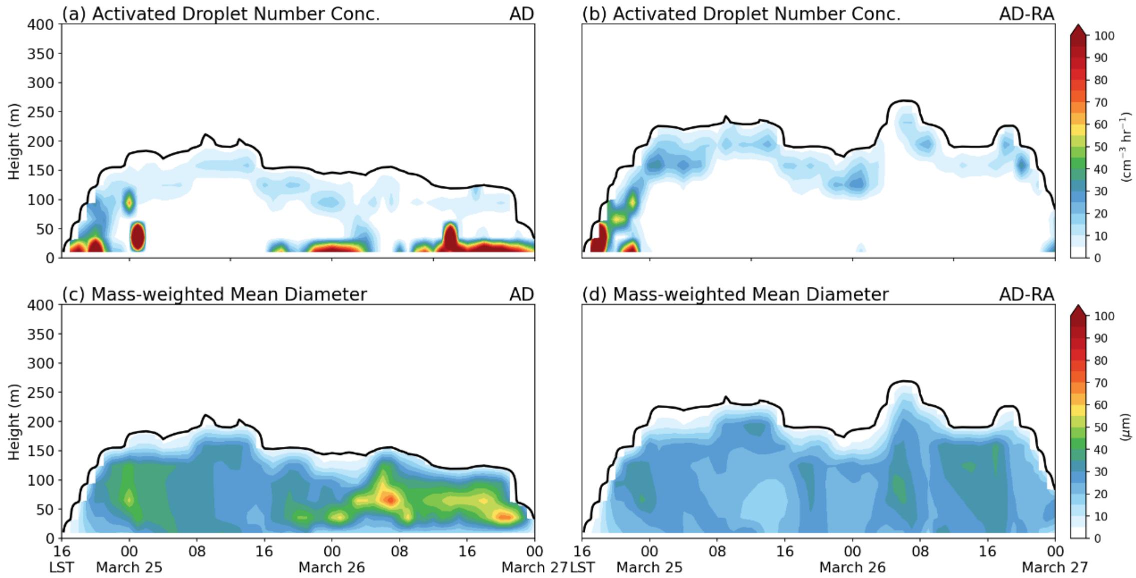

Figure S9. Area-averaged time-height distributions of (a, b) activated droplet number concentration (shaded in cm^{-3} hr^{-1}) and (c, d) mass-weighted mean diameter (shaded in μm) over the region marked by the gray rectangles in Fig. S5. The left and right columns correspond to the AD and AD-RA experiments. Black contours denote the LWC threshold of 0.016 g m^{-3}.

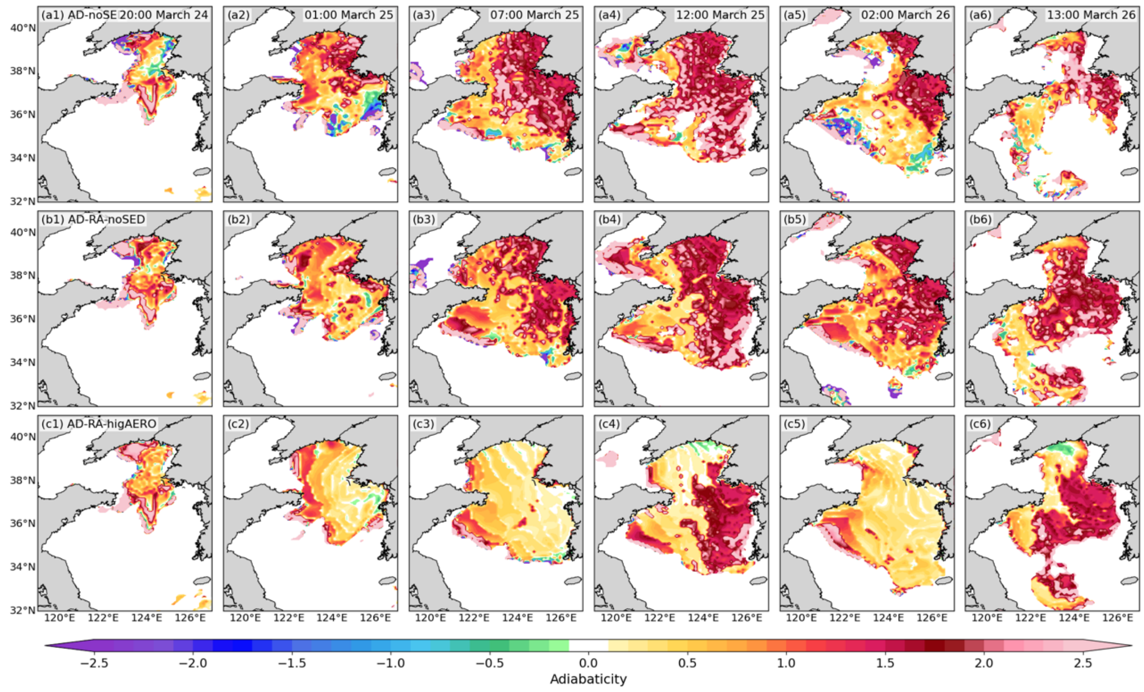

Figure S10. Simulated adiabaticity (shading in unit 1) from the (row a) AD-noSED, (b) AD-RA-noSED, and (c) AD-RA-higAERO experiments, respectively. Columns 1-6 correspond to 20:00 LST on March 24, 01:00, 07:00, and 12:00 LST on March 25, and 02:00 and 13:00 LST on March 26, respectively.

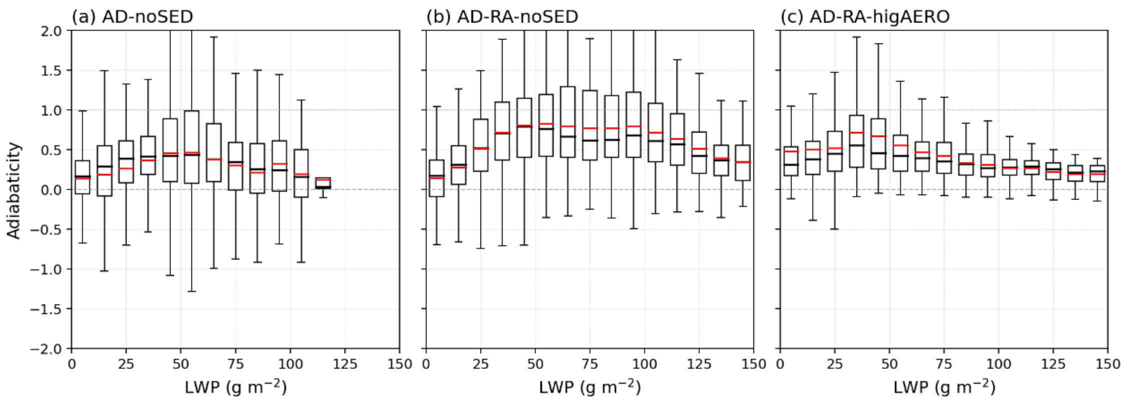

Figure S11. Boxplots of the adiabaticity for different LWP ranges for the (a) AD-noSED, (b) AD-RA-noSED, and (c) AD-RA-higAERO experiments during 16:00 LST March 24 to 00:00 LST March 27. Samples are taken from oceanic grid points within the 121-127° E, 33-40° N region and are grouped into 10 g m^{-2} LWP bins. Only samples with lowest-level LWC exceeds 0.016 g m^{-3} are included. Each box denotes the 25th and 75th percentiles, with the black line indicating the median and the red line indicating the mean. The whiskers extend to the minimum and maximum values within 1.5 times the interquartile range. The dashed and dotted horizontal lines indicate adiabaticity values of 0 and 1, respectively.

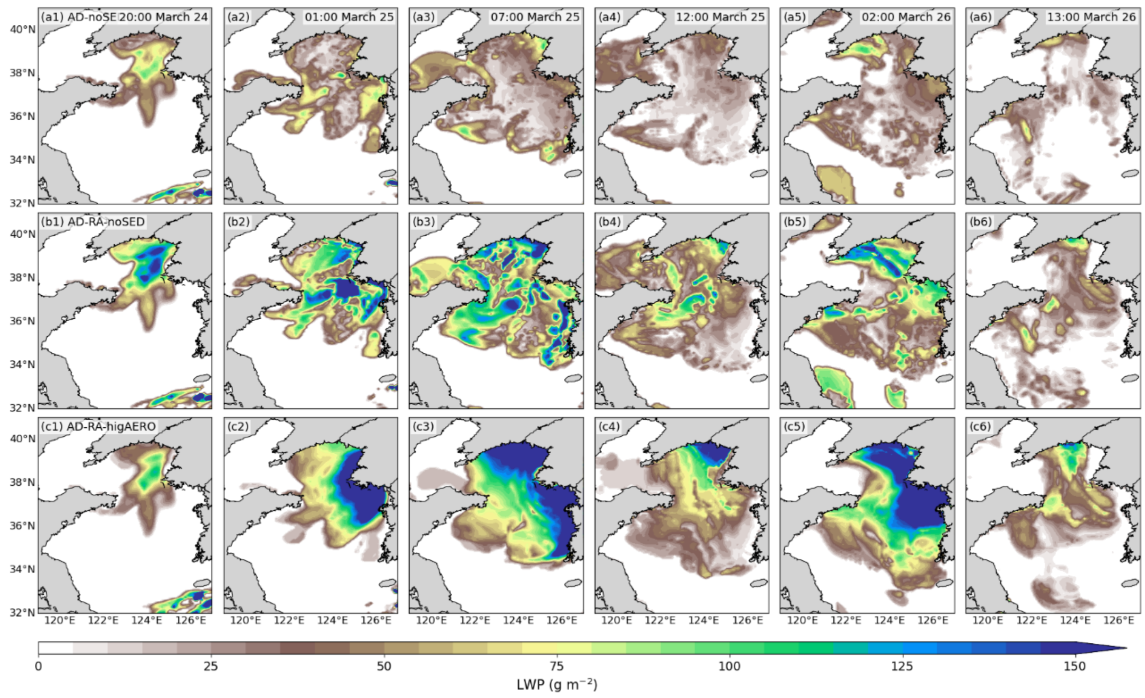

Figure S12. Liquid water path (shaded in g m^{-2}) for the (row a) AD-noSED, (b) AD-RA-noSED, and (c) AD-RA-higAERO experiments. Columns 1-6 correspond to 20:00 LST on March 24, 01:00, 07:00, and 12:00 LST on March 25, and 02:00 and 13:00 LST on March 26, respectively.